7. J. Bonache, F. Martin, F. Falcone, et al., Application of complementary split-ring resonators to the design of compact narrow band-pass structures in microstrip technology, Microwave Opt Technol Lett 5 (2005), 508-512.
8. J. Bonache, F. Martin, I. Gil, J. Garcia-Garcia, Novel microstrip filters based on complementary split rings resonators, IEEE Trans Microwave Theory Tech 1 (2006), 265-271.

PHOTOREFRACTIVE PROPERTIES OF DOUBLE-DOPED HF:CE:LINBO$_3$ CRYSTALS

Wei Zhou[1], Biao Wang[1], Wei Yuan[2], Furi Ling[1], Decai Ma[2], and Yiran Nie[2]
[1]School of Physics Science and Engineering, Sun Yat-Sen University, Guangzhou 510275, China; Corresponding author: zhouweijupiter@yahoo.com.cn
[2]School of Astronautics, Harbin Institute of Technology, Harbin 150001, China

Received 21 October 2007

ABSTRACT: *In this article, the double-doped Hf:Ce:LiNbO$_3$ crystals were grown by the Czochralski method and its photorefractive properties were systematically studied. Samples were treated with different oxidation/reduction. The photorefractive properties of Hf:Ce:LiNbO$_3$ crystals were investigated by the two-beam coupling method. The results shown that the photorefractive properties of Hf:Ce:LiNbO$_3$ crystals were improved as compared with that of Ce:LiNbO$_3$ crystals. The oxidation/reduction treatment had great effect on the photorefractive properties and the doping mechanism was also discussed.* © 2008 Wiley Periodicals, Inc. Microwave Opt Technol Lett 50: 1693–1695, 2008; Published online in Wiley InterScience (www.interscience.wiley.com). DOI 10.1002/mop.23448

Key words: *Hf:Ce:LiNbO$_3$ crystal; photorefractive property; oxidation/reduction treatment*

1. INTRODUCTION

Lithium niobate ($LiNbO_3$, LN) single crystal has been extensively studied because of its excellent ferroelectric, piezoelectric, and photorefractive properties, which is one of the promising candidates for holographic data storage. The photorefractive properties of the LN can be effectively affected by doping with transition metal and rare earth ions, such as Fe [1], Cu [2], Cr [3], Mn [4], Sc [5], Ce [6], Zn [7], Pr [8], Nd [9]. The photorefractive sensitivity of Ce:$LiNbO_3$ is one order higher than that of congruent undoped $LiNbO_3$ [6]. But low optical damage resistance ability and long response time are the two main disadvantages of Ce:$LiNbO_3$. Doping with damage-resistance dopants is found to be an effective way to solve the problem [10]. Sc [5], Zn [7], Mg [11], In [12], and Hf [13-15] have been used to increase the optical damage resistance ability of $LiNbO_3$. In addition, modest oxidation or reduction can change the valance state of the doping ions and affect the photorefractive properties of the crystal.

In this article, Hf was employed to enhance the optical damage resistance ability of Ce:$LiNbO_3$. Oxidation/reduction treatments were adopted to change the photorefractive properties. The photorefractive properties of Hf:Ce:$LiNbO_3$ were discussed in detail.

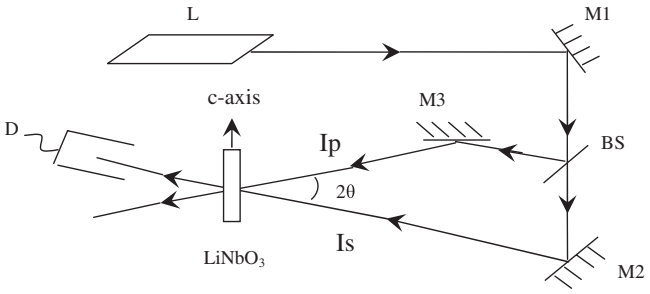

Figure 1 Experiment setup of the two-beam coupling method

2. CRYSTAL GROWTH AND SAMPLE PREPARATION

The $LiNbO_3$ crystals doped with 0.1 wt% CeO_2 and 4 mol% HfO_2 were grown by the Czochralski method along the c-axis from the congruent melt. The Ce:$LiNbO_3$ were grown for comparison. The raw materials were ultra-pure. After precisely weighed and thoroughly mixed, the materials were calcined at 750°C and then sintered at 1150°C for 4 h, respectively. The composition of the raw materials was shown in Table 1.

The $LiNbO_3$ crystals were grown with the pulling rate of 1 ~ 2 mm/h and rotation rate of 15 ~ 25 rpm in air. The temperature gradient above the melt was 30 ~ 40°C/cm. After growth, the crystals were polarized at 1200°C with DC current density of 5 mA/cm^2 for 30 mins. Then the polarized crystals were cut to the size of 10 mm × 2 mm ×10 mm (a × b × c). Finally the crystals were polished to optical grade.

The powders of Li_2CO_3 and Nb_2O_5 were chosen as the reducing and oxidizing agents, respectively. The reduction treatment was carried out by burying the samples into Li_2CO_3 powder, heated up to 550°C and hold for 24 h; likewise, the oxidation treatment was burying the samples into Nb_2O_5 powder, then heated up to 1150°C and hold for 12 h.

3. MEASUREMENT OF PHOTOREFRACTIVE PROPERTIES

The photorefractive properties of the crystals (diffraction efficiency, response time, and exponential gain coefficient) were measured by the two-beam coupling method. The experimental setup was shown in Figure 1. Both a signal beam and a pump beam originated from an Ar^+ laser (λ = 514.5 nm) irradiated on a sample with polarization direction parallel to the *c*-axis of the sample. The diameters of both the pump beam and the signal beam were adjusted to 1 mm. The intensity ratio between them was

TABLE 1 Composition of the Raw Materials

Crystal No.	1	2	3	4	5	6
CeO_2 (wt%)	0.1	0.1	0.1	0.1	0.1	0.1
HfO_2 (mol%)	0	0	0	4	4	4
Crystal size (mm^2)	Φ30 × 30	Φ30 ×30	Φ30 × 30	Φ30 × 25	Φ30 × 25	Φ30 × 25
Sample size (mm^3)	10 × 2 × 10	10 × 2 × 10	10 × 2 × 10	10 × 2 × 10	10 × 2 × 10	10 × 2 × 10
Treatment	As grown	Reduction	Oxidation	As grown	Reduction	Oxidation

TABLE 2 The Diffraction Efficiency η and Response Time τ of the Crystals

Crystal No.	(%)	
1	58	170
2	53	128
3	60	226
4	42	23
5	39	12
6	48	37

1860. The external crossing angle of the two beams was designed as 2θ.

Diffraction efficiency η is defined as the ratio of the diffraction light intensity I_1' to the transmission light intensity I_1 ,

$$\eta = \frac{I_1'}{I_1} \times 100\% \tag{1}$$

The response time τ is defined as the time interval that is from the time of the incident light begins irradiating on the crystal to the time when the diffraction efficiency reaches $(1\text{-}e^{-1})$ of its maximum.

The exponential gain coefficient is one of the important indicators to evaluate the photorefractive properties of the photorefractive crystal, which corresponds to the energy transition from the pump light to the signal light during the information storage process. The exponential gain coefficient Γ is defined as

$$\Gamma = \frac{1}{\delta}\ln\frac{I_s' I_p}{I_s I_p'} \approx \frac{1}{\delta}\ln\frac{I_s'}{I_s} \tag{2}$$

where I_s' and I_p' (I_s and I_p) are the transmitted intensities of signal beam and pumping beam with (without) coupling, respectively, and δ is the thickness of the sample. When the intensity of the pump beam is much larger than that of the signal beam, the exponential gain coefficient becomes independent of the pump beam intensity (i.e. $I_p \approx I_p'$).

4. RESULTS AND DISCUSSIONS

The results were shown in Table 2 and Figure 2. It was obvious that the response time τ of Hf:Ce:$LiNbO_3$ was greatly shortened than that of Ce:$LiNbO_3$. After reduction treatment, the diffraction efficiency η of the crystals decreased and the response time τ was shortened, but the exponential gain coefficient Γ increased. On the contrary, the diffraction efficiency η and the response time τ of the oxidized crystals increased, but the exponential gain coefficient Γ decreased.

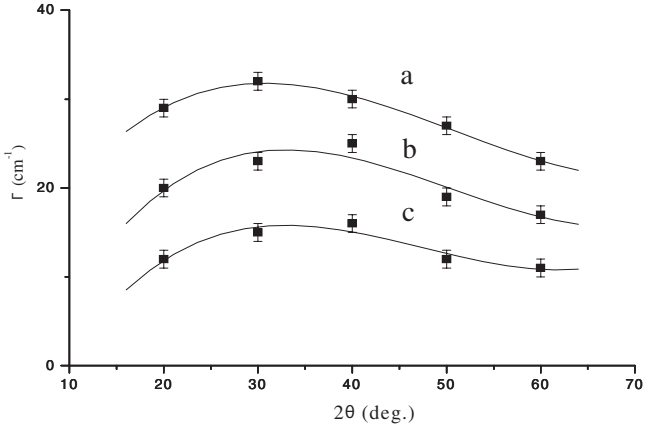

Figure 2 Experimental curves of $\Gamma \sim 2\theta$. (a) No.5 sample of Hf:Ce:$LiNbO_3$ with reduction treatment. (b) No.4 sample of Hf:Ce:$LiNbO_3$. (a) No.6 sample of Hf:Ce:$LiNbO_3$ with oxidation treatment

The response time τ could be expressed as [16]

$$\tau = \frac{\varepsilon\varepsilon_0}{\sigma_{ph} + \sigma_d} \tag{3}$$

where ε and ε_0 were the relative dielectric constant and the dielectric constant in vacuum, respectively. ε was taken as 32 [16]. σ_{ph} and σ_d were photoconductivity and dark conductivity, respectively. In the range of our measurement, σ_d could be negligible because $\sigma_d \ll \sigma_{ph}$. According to Li vacancy model [17], there were lots of Nb_{Li} (Nb atom on the Li vacancy) in congruent $LiNbO_3$ crystals which acted as electron trap centers. In Hf:Ce:$LiNbO_3$, the Nb_{Li} decreased as the Hf doping concentration increased, and it was cleared up as the concentration of Hf achieved 4 mol%. So σ_{ph} increased and the response time of Hf:Ce:$LiNbO_3$ was greatly shortened.

Further more, oxidation/reduction could affect the concentrations of the electron donor and acceptor. The concentrations of the lower valence Ce^{3+} and the oxygen vacancy (Vo +2e) increased after reduction. They gave out electrons when the laser irradiated on the crystal, so the σ_{ph} increased and the photorefractive performance of the crystal was enhanced though the diffraction efficiency was little decreased.

5. CONCLUSION

The photorefractive properties of Hf:Ce:$LiNbO_3$ were enhanced as compared with that of Ce:$LiNbO_3$. The oxidation/reduction treatment had significant effect on the photorefractive properties. The reduced Hf:Ce:$LiNbO_3$ showed favorable photorefractive properties and was a promising holographic storage media.

ACKNOWLEDGMENT

This work was supported by the National Natural Science Foundation of China (10572155, 10172030, 10732100′50232030) and The Science Foundation of Guangdong Province (2005A10602002).

REFERENCES

1. Y.P. Yang, I. Nee, K. Buse, and D. Psaltis, Ionic and electronic dark decay of holograms in $LiNbO_3$:Fe crystals, Appl Phys Lett 78 (2001), 4076–4078.
2. X.W. Xu, X.N Liang, T.C. Chong, S.N Yuan, S. Solanki, and Y. Tay, Vertical bridgman growth and optical characterization of $LiNbO_3$: Cu:Ce crystals, J Cryst Growth 275 (2005), e791–e797.
3. K. Chah, M. Aillerie, M.D. Fontana, G.I. Malovichko, K. Betzler, and E. Kokanyan, Influence of chromium doping on the electro-optic properties of lithium niobate, Opt Commun 136 (1997), 231–234.
4. Z.J. Sun, H.T. Li, W. Cai, and L.C. Zhao, Studies of photorefractive fields of MnO and Fe_2O_3 co-doped near stoichiometric $LiNbO_3$ crystals, Opt Mater 27 (2005), 1560–1562.
5. J.K. Yamamoto, K. Kitamura, N. Iyi, S. Kimura, Y. Furukawa, and M. Sato, Increased optical damage resistance in Sc_2O_3-doped $LiNbO_3$, Appl Phys Lett 61 (1992), 2156–2158.
6. G.H. Jin, M.H. Li, G.R. Sun, Y.H. Xu, and Y.K. Gao, Growth of Ce:$LiNbO_3$ crystal and research of phase conjugation, J Synthetic Cryst 21 (1992), 362–366.
7. T.R. Volk, N.V. Razumovski, A.V. Mamaev, and N.M. Rubinina, Hologram recording in Zn-doped $LiNbO_3$ crystals, J Opt Soc Am B: Opt Phys 13 (1996), 1457–1460.
8. R.M. Macfarlane, Y. Sun, F. Konz, and R.L. Cone, Inhomogeneous and homogeneous broadening in Pr^{3+} and Er^{3+} doped lithium niobate,

Pacific Rim Conference on Lasers and Electro-Optics, CLEO Tech Dig (2000), 492–493.
9. J.W. Shur, and D.H. Yoon, Fluorescence properties of Nd^{3+} doped stoichiometric $LiNbO_3$ fiber single crystals by micro-pulling down method, Cryst Res Technol 39 (2004), 1099–1103.
10. G.Q. Zhang, G.Y. Zhang, S.M. Liu, J.J. Xu, Q. Sun, and X.Z. Zhang, The threshold effect of incident light intensity for the photorefractive light-induced scattering in $LiNbO_3$:Fe,M (M=Mg^{2+}, Zn^{2+}, In^{3+}) crystals, J Appl Phys 83 (1998) 4392–4396.
11. B.C. Grabmaier, and F. Otto, Growth and investigation of MgO-doped $LiNbO_3$, J Cryst Growth 79 (1986), 682–688.
12. Y.F. Kong, J.K. Wen, and H.F. Wang, New doped lithium niobate crystal with high resistance to photorefraction-$LiNbO_3$:In, Appl Phys Lett 66 (1995), 280–281.
13. L. Razzari, P. Minzioni, I. Cristiani, V. Degiorgio, and E.P. Kokanyan, Photorefractivity of hafnium-doped congruent lithium-niobate crystals, Appl Phys Lett 86 (2005), 131914.
14. E.P. Kokanyan, L. Razzari, I. Cristiani, V. Degiorgio, and J.B. Gruber, Reduced photorefraction in hafnium-doped single-domain and periodically poled lithium niobate crystals, Appl Phys Lett 84 (2004), 1880–1882.
15. S.Q. Li, S.G. Liu, Y.F. Kong, J.J. Xu, and G.Y. Zhang, Enhanced photorefractive properties of $LiNbO_3$:Fe crystals by HfO_2 codoping, Appl Phys Lett 89 (2006), 101126.
16. S.M. Kostritskii, and O.G. Sevostyanov, Influence of intrinsic defects on light-induced changes in the refractive index of lithium niobate crystals, Appl Phys B 65 (1997), 527–533.
17. P. Lerner, C. Legras, and J. P. Dumas, Stoechiométrie des monocristaux de méta-niobate de lithium, J Cryst Growth 3-4 (1968), 231–235.

A NOVEL DUAL-FREQUENCY UNEQUAL WILKINSON POWER DIVIDER

Cong Feng, Gang Zhao, Xu-Feng Liu, and Fu-Shun Zhang
National Key Laboratory of Antennas and Microwave Technology, Xidian University, Xi'an, 710071, People's Republic of China; Corresponding author: fengcong1984@163.com

Received 22 October 2007

ABSTRACT: *This article presents the design of a novel dual-frequency unequal Wilkinson power divider. This unequal power divider fulfills an arbitrary power split and all the other features of a conventional Wilkinson unequal power divider simultaneously at two arbitrary frequencies. The structure of this power divider and the formulas used to determine the design parameters have been given. Both simulated and measured results of the dual-frequency unequal Wilkinson power divider are presented to validate our proposed idea. Good experimental performances of the proposed power divider, including an arbitrary power split and a good isolation between the output ports at both frequencies are obtained.* © 2008 Wiley Periodicals, Inc. Microwave Opt Technol Lett 50: 1695–1699, 2008; Published online in Wiley InterScience (www.interscience.wiley.com). DOI 10.1002/mop.23447

1. INTRODUCTION

The power divider is one of the most popular passive circuits used for microwave and millimeter-wave applications. In a very recent publication [1], a dual-frequency unequal power divider has been presented. A suitable optimization procedure was applied using genetic algorithms in order to satisfy several requirements at both frequencies. This power divider was designed by numerical solution, which, although not analytically exact, was numerically nearly exact. Here, we present a true exact solution to the dual-frequency unequal power divider with a dual-band transformer section, which has been introduced by Monzon in [2]. A dual-frequency equal Wilkinson power divider with this transformer section has been reported in [3], the authors used the even and odd mode analysis to determine the circuit parameters. But for considering the special requirements of the dual-frequency transformer section, and the unique characteristic of the unequal power divider, there is still no exact solution to the dual-frequency unequal power divider. Therefore, we present an extension of Monzon's analysis to the design of a dual-frequency unequal power divider. The proposed power divider operates at two arbitrary frequencies of interest f_1 and f_2, and at an arbitrary power split. The design parameters of the dual-frequency unequal Wilkinson power divider are presented in explicit closed form. The validity of this analysis is demonstrated by experimental results with a power split of 2:1 and a power split of 1.5:1 at 0.9 GHz and 1.8 GHz, which are applied in present global system for mobile communication (GSM) and personal communication system (PCS), and with a power split of 2:1 at 0.915 GHz and 2.45 GHz, which are applied in RFID.

2. THEORY AND DESIGN EQUATIONS

In a conventional Wilkinson unequal power divider, the output ports are shunted with a parallel connection of a resistor R. If the power split at Ports 2 and 3 is $K^2 = P_3/P_2$, we can consider that the output ports are matching with the impedance $R_2 = Z_0K$ and $R_3 = Z_0/K$ [4], where Z_0 is the reference impedance. The characteristic impedance of each branch and the resistor R are given by [4]:

$$Z_{03} = Z_0\sqrt{\frac{1+K^2}{K^3}} \tag{1}$$

$$Z_{02} = K^2Z_{03} = Z_0\sqrt{K(1+K^2)} \tag{2}$$

$$R = Z_0\left(K+\frac{1}{K}\right) \tag{3}$$

This conventional Wilkinson unequal power divider operates at one design frequency f_1 and at all its odd harmonics. Therefore, it is not suitable for some dual-band operations. In 2003, a small dual-frequency transformer section has been introduced by Monzon in [2], which could operate at any two arbitrary f_1 and f_2. For using Monzon's Theory in the design of a dual-frequency unequal power divider, each quarter-wave branch of a conventional Wilkinson unequal power divider is substituted by transformer in two sections with the characteristic impedance of Z_1 and Z_2 and the length of L, respectively. A schematic diagram of the proposed Wilkinson unequal power divider, which operates at two arbitrary frequencies and at an arbitrary power split, is shown in Figure 1.

When Monzon's Theory is applied, it is necessary to determine the input and output impedance of each branch in the unequal power divider. In a conventional unequal Wilkinson power divider, each branch is a $\lambda/4$ transformer section. Assuming that the characteristic impedance of this section is Z_0, we can obtain Z_{in} as

$$Z_{in} = Z_0^2/Z_{out} \tag{4}$$

By using (1) and (2) in (4), with $Z_{out2} = R_2 = Z_0K$ and $Z_{out3} = R_3 = Z_0/K$, respectively, Z_{ina} and Z_{inb} can be obtained as

$$Z_{ina} = Z_0(1+K^2) \tag{5}$$

$$Z_{inb} = Z_0\left(1+\frac{1}{K^2}\right) \tag{6}$$